

## BRIEF COMMUNICATION

# Synthesis of New Bimetallic Transition Metal Oxynitrides V–Me–O–N (Me = Mo and W) by Temperature-Programmed Reaction

C. Charles Yu and S. Ted Oyama

*Department of Chemical Engineering, Virginia Polytechnic Institute and State University, Blacksburg, Virginia 24061*

Received July 19, 1994; in revised form September 16, 1994; accepted September 21, 1994

Transition metal carbides and nitrides have attracted attention as possible replacements for platinum group catalysts. Most of the work has been carried out with single-metal compounds. We report here the preparation of two new bimetallic compounds, V–Mo and V–W oxynitrides, obtained by nitridding oxide precursors with ammonia gas via a temperature-programmed reaction. The bimetallic oxide precursors are prepared by conventional solid state reaction using commercial V, Mo, and W oxides. The oxynitrides thus obtained adopt a face-centered cubic crystal structure. They have high specific surface areas (74 and 62 m<sup>2</sup> g<sup>-1</sup>), and their pyrophoricity suggests high surface activity. © 1995 Academic Press, Inc.

Nitride formation is very common among transition elements of the first row and the early members of the second and third rows. In general, transition metal nitrides have physical properties characteristic of refractory ceramics, with very high melting points, hardnesses, and tensile strengths. At the same time, they display electronic and magnetic properties resembling those of metals, such as electrical conductivity, Hall coefficient, magnetic susceptibility, and heat capacity (1, 2).

Transition metal nitrides are used as cutting tools, wear-resistant parts, high-temperature structural materials (3, 4), electronic and magnetic components (5–8), and superconductors (9, 10). In addition, they have received considerable attention as catalysts due to their resemblance to the noble Group VIII metals (Pt, Pd, Rh, etc.) in chemical properties (11, 12).

In recent years a number of bimetallic nitrides and oxynitrides combining transition metals with alkali (13, 14), alkaline earth (15), and lanthanide (16) elements have been reported (17–19). In comparison, few bimetallic nitrides or oxynitrides with only transition metals have been synthesized and fully characterized. Among these are CuWN<sub>2</sub> (18), FeWN<sub>2</sub> (20), and Ni<sub>3</sub>Mo<sub>3</sub>N (21). The oxynitrides

reported here are related to CuWN<sub>2</sub> and FeWN<sub>2</sub> in that they have high concentrations of the nonmetal elements, but have cubic instead of hexagonal structure.

Bimetallic nitrides and oxynitrides containing strongly electropositive elements (e.g., LiMoN<sub>2</sub>, Li<sub>3</sub>FeN<sub>2</sub>, CaCrN<sub>3</sub>, LaTaON<sub>2</sub>) have substantial ionic character and their limiting compositions have been described by the normal rules of valency (–2 for O, –3 for N) (20). This is not the case for the pure transition metal compounds, which are metallic in nature. Their phases can exist over broad composition ranges with appreciable vacancy concentrations (both metal and nonmetal), and their physical properties are quite sensitive to composition. It is expected that the partial replacement of nitrogen by oxygen and, at the same time, partial substitution of one transition metal for another can alter the properties substantially.

V–Mo–O–N and V–W–O–N were prepared by temperature-programmed reaction (TPR), a technique developed in the early 1980s which produces nitrides with high specific surface area (22, 23). The current TPR approach involves placing a bimetallic oxide precursor in a flowing ammonia stream while raising the temperature in a controlled manner. The bimetallic oxide precursors were prepared by solid state reaction of two monometallic oxides. Because the free energy of formation of such ternary oxides is small (17), thermodynamic calculations (17) could not be used to predict the feasibility of nitridation.

The vanadium–molybdenum oxide was prepared by first mixing vanadium(V) oxide (V<sub>2</sub>O<sub>5</sub>, 99.9%, Johnson Matthey) and molybdenum(VI) oxide (MoO<sub>3</sub>, 99.95%, Johnson Matthey) at a V:Mo ratio of 2:1. The mixture was thoroughly ground, pressed into pellets, and then fired in air at 948 K for 6 hr. After cooling to room temperature, the pellets were pulverized into fine powders. The product had a dark green color, and XRD analysis indicated that it was V<sub>2</sub>MoO<sub>8</sub> (JCPDS card 20-1377). The

vanadium–tungsten oxide was prepared in a similar manner with a V : W ratio of 1 : 1 and was fired at 1323 K for 6 hr. The product had a green color, and the absence of its XRD pattern from the JCPDS files suggested that it was a new compound. The XRD pattern showed neither a match to any existing vanadium–tungsten oxide files nor evidence of any peaks due to vanadium or tungsten monometallic oxides.

For the TPR process the  $V_2MoO_8$  and  $VWO_x$  powders were transferred to a quartz reactor, which was placed inside a tubular resistance furnace. An ammonia gas stream was passed through the oxide powders at a flow rate of  $6.82 \times 10^2 \mu\text{mole sec}^{-1}$  ( $1000 \text{ cm}^3/\text{min}$ ). The temperature of the reactor was increased at a linear rate of  $8.3 \times 10^{-2} \text{ K sec}^{-1}$  (5 K/min) to a final temperature ( $T_{\text{max}}$ ) which was held for a period of time ( $t_{\text{hold}}$ ).  $T_{\text{max}}$  and  $t_{\text{hold}}$  were 1037 K and 30 min for V–Mo–O–N, and 1009 K and 110 min for V–W–O–N. At the end of the temperature-programmed reaction, the samples were removed from the furnace to quench them to room temperature and the flow of ammonia gas was switched to helium. The products thus obtained were extremely pyrophoric and needed to be passivated before exposure to air. To passivate the samples, pure helium gas was switched to a gas mixture containing 0.5%  $O_2$  in helium at a flow rate of  $24 \mu\text{mole sec}^{-1}$  ( $35 \text{ cm}^3/\text{min}$ ). The purpose of passivation was to safely cover the active surface with a layer of oxygen to prevent oxidation of the bulk. The time of passivation was set to 3 hr per gram of starting bimetallic oxide. The passivated samples were characterized by XRD analysis, inductively coupled plasma (ICP) elemental analysis, and nitrogen adsorption. XRD analysis was carried out using a powder diffractometer (Siemens Model D 500 with a  $CuK\alpha$  monochromatized radiation source). Nitrogen adsorption was measured by a pulse technique with a 30%  $N_2$  in He gas mixture. The surface areas of the samples were determined by the single point BET method. The crystallite sizes of the samples were calculated by the Scherrer equation based on XRD peak broadening and compared with the particle size derived from the surface area measurements.

Elemental analysis of the two bimetallic oxynitrides gave the chemical formulas  $V_{2.0}Mo_{1.0}O_{1.7}N_{2.4}$  and  $V_{1.0}W_{1.4}O_{2.7}N_{2.5}$ . The error in analysis for the metals was less than 10%. Further studies indicated that the sample nitrogen content could be altered by changing reaction conditions. Increasing the maximum temperature and/or the final soaking time of the TPR process resulted in higher nitrogen content. However, higher reaction temperature normally led to samples of lower surface area. In the V–W system, the deviation of the V to W ratio (1.0 : 1.4 in the final oxynitride compared to 1.0 : 1.0 for the starting material) could be caused by sublimation during the high-temperature (1323 K) bimetallic oxide synthesis. The

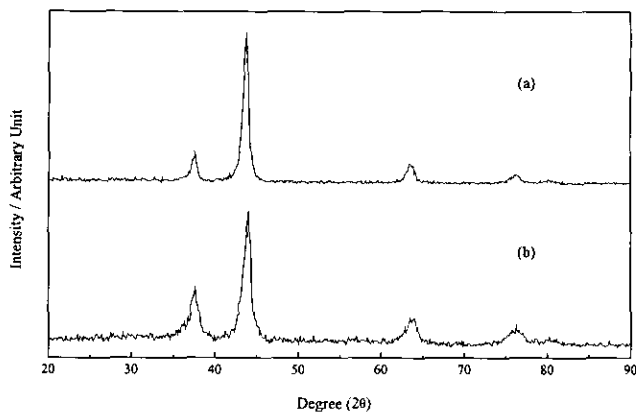


FIG. 1. XRD patterns of (a)  $V_{2.0}Mo_{1.0}O_{1.7}N_{2.4}$  and (b)  $V_{1.0}W_{1.4}O_{2.7}N_{2.5}$ .

melting point of  $V_2O_5$  is only 963 K, whereas that of  $WO_3$  is 1473 K. At 1323 K, the corresponding vapor pressure of  $V_2O_5$  is 64 Pa (0.48 Torr) while that of  $WO_3$  is 0.14 Pa (0.0011 Torr) (24). Both oxynitride samples contain substantial amounts of oxygen, and we suspect that this is partly due to the oxide layer deposited on the surface. The crystallites have a very large surface area to volume ratio.

Figure 1 shows the X-ray diffraction patterns of both  $V_{2.0}Mo_{1.0}O_{1.7}N_{2.4}$  and  $V_{1.0}W_{1.4}O_{2.7}N_{2.5}$ . Both samples reported here have the same characteristic pattern of the rock salt structure (space group  $Fm\bar{3}m$ ), in which the metal atoms randomly occupy a face centered cubic (fcc) lattice. The peaks (only four of the five peaks are clearly visible in the scale presented) could be indexed as (111), (200), (220), (311), and (222) reflections, giving for  $V_{2.0}Mo_{1.0}O_{1.7}N_{2.4}$  the lattice parameter  $a = 0.413 \text{ nm}$  and for  $V_{1.0}W_{1.4}O_{2.7}N_{2.5}$ ,  $a = 0.414 \text{ nm}$ . Another distinctive feature of the two XRD patterns, other than their simplicity, is the unusual broadening of the peaks. The crystallite size ( $D_c$ ), calculated by the Scherrer equation, indicates dimensions of 11 nm for  $V_{2.0}Mo_{1.0}O_{1.7}N_{2.4}$  and 6.7 nm for  $V_{1.0}W_{1.4}O_{2.7}N_{2.5}$ . The results are consistent with the high specific surface area values ( $S_g$ ),  $74 \text{ m}^2 \text{ g}^{-1}$  for  $V_{2.0}Mo_{1.0}O_{1.7}N_{2.4}$  and  $62 \text{ m}^2 \text{ g}^{-1}$  for  $V_{1.0}W_{1.4}O_{2.7}N_{2.5}$ , which correspond to particle sizes of 7.9 and 5.1 nm. The particle size ( $D_p$ ) can be calculated from the equation  $D_p = 6 / (S_g \rho)$ , where  $\rho$  is taken to be  $10.2 \text{ g cm}^{-3}$  for the molybdenum oxynitride compound and  $18.9 \text{ g cm}^{-3}$  for the tungsten oxynitride compound, assuming perfect rock salt structures for such compounds. Table 1 summarizes the surface area and  $D_c$  and  $D_p$  values of  $V_{2.0}Mo_{1.0}O_{1.7}N_{2.4}$  and  $V_{1.0}W_{1.4}O_{2.7}N_{2.5}$ . Good agreement exists for  $D_p$  and  $D_c$ , indicating that the particles are not polycrystalline aggregates.

$V_{2.0}Mo_{1.0}O_{1.7}N_{2.4}$  and  $V_{1.0}W_{1.4}O_{2.7}N_{2.5}$  are two members of a new bimetallic transition metal oxynitride class. Their

TABLE 1  
Characteristics of Bimetallic Oxynitrides V-M-O-N

Sample	Surface area $S_g(\text{m}^2 \text{g}^{-1})$	Crystallite size $D_c(\text{nm})$	Particle size $D_p(\text{nm})$	Lattice parameter $a(\text{nm})$
V-Mo-O-N	74	11	7.9	0.413
V-W-O-N	62	6.7	5.1	0.414

highly pyrophoric characteristic, which indicates high reactivity, combined with their high surface area makes them very interesting materials. Further studies on their surface chemistry and reactivity are in progress.

#### ACKNOWLEDGMENTS

This paper was written with support from Akzo Nobel and the U.S. Department of Energy.

#### REFERENCES

- L. E. Toth, "Transition Metal Carbides and Nitrides." Academic Press, New York, 1971.
- S. T. Oyama, *J. Solid State Chem.* **96**, 442 (1992).
- G. V. Samsonov, in "Refractory Transition Metal Compounds: High Temperature Cermets." Academic Press, New York/London, 1964
- M. Molarius, A. S. Korhonen, and E. O. Ristolainen, *J. Vac. Sci. Technol. A* **3**, 2419 (1985).
- M. Mekata, *J. Phys. Soc. Jpn.* **17**, 796 (1962).
- T. K. Tim and M. Takahashi, *Appl. Phys. Lett.* **20**, 492 (1972).
- K. Tagawa, E. Kita, and A. Tasaki, *Jpn. J. Appl. Phys.* **21**, 1596 (1982).
- N. Kumar, J. T. McGinn, K. Pourrezaei, B. Lee, and C. Douglas, *J. Vac. Sci. Technol. A* **6**, 1602 (1988).
- T. H. Courtney, J. Reintjes, and J. Wulff, *J. Appl. Phys.* **36**, 660 (1965).
- Y. M. Shy, L. E. Toth, and R. Somasundaram, *J. Appl. Phys.* **44**, 5539 (1973).
- S. T. Oyama and G. L. Haller, *Catalysis, Spec. Period. Rep.* **5**, 333 (1981).
- S. T. Oyama, *Catal. Today* **15**, 179 (1992).
- S. H. Elder, L. H. Doerrer, F. J. DiSalvo, J. B. Parise, D. Guyomard, and J. M. Tarascon, *Chem. Mater.* **4**, 928 (1992).
- A. Gudat, R. Kniep, A. Rabenau, W. Bronger, and U. Ruschewitz, *J. Less-Common Met.* **161**, 31 (1990).
- D. A. Vennos, M. E. Badding, and F. J. DiSalvo, *Inorg. Chem.* **29**, 4059 (1990).
- R. Marchand, F. Pors, and Y. Laurent, *Ann. Chim. (Paris)* **16**, 553 (1991).
- S. H. Elder, F. J. DiSalvo, L. Topor, and A. Navrotsky, *Chem. Mater.* **5**, 1545 (1993).
- U. Zachwieja and H. Jacobs, *Eur. J. Solid State Inorg. Chem.* **28**, 1055 (1991).
- T. Yamamoto, S. Kikkawa, and F. Kanamaru, *Solid State Ionics* **63-65**, 148 (1993).
- D. S. Bem and H.-C. Zur Loye, *J. Solid State Chem.* **104**, 467 (1993).
- D. S. Bem, C. P. Gibson, and H.-C. Zur Loye, *Chem. Mater.* **5**, 397 (1993).
- L. Volpe and M. Boudart, *J. Solid State Chem.* **59**, 332 (1985).
- S. T. Oyama, Ph.D. Dissertation. Stanford University, 1981.
- G. V. Samsonov, "The Oxide Handbook" (translated by C. N. Turton and T. I. Turton). IFI/Plenum, New York, 1973.

## BRIEF COMMUNICATION

On  $\text{CuCrP}_2\text{S}_6$ : Copper Disorder, Stacking Distortions, and Magnetic OrderingV. Maisonneuve, C. Payen, and V. B. Cajipe<sup>1</sup>*Institut des Matériaux de Nantes, CNRS-UMR 110, 2, rue de la Houssinière, 44072 Nantes Cedex 03, France*

Received June 6, 1994; accepted September 29, 1994

The pseudo-one-particle potential for  $\text{Cu}^I$  in  $\text{CuCrP}_2\text{S}_6$  was calculated from the room temperature (RT) structural model and shown to have a double-well shape straddling the center of the  $\text{CuS}_6$  octahedron. It is argued that this finding supports the thermal hopping interpretation of the RT copper disorder in this compound. The RT monoclinic unit cell parameters were also re-measured and found to be consistent with the presence of out-of-plane packing deformations. Last, the antiferromagnetic structure of the  $\text{Cr}^{III}$  moments below  $T_N \approx 30$  K was determined using neutron powder diffraction. © 1995 Academic Press, Inc.

The room temperature (RT) structure and magnetic study of  $\text{CuCrP}_2\text{S}_6$  published by Colombet *et al.* (1) gave the first example of an unusually extended electronic density associated with the monovalent cation in a lamellar  $M^I M'^{III} \text{P}_2\text{S}_6$  phase ( $M = \text{Ag, Cu, and } M' = \text{V, Cr, In, Sc}$ ) (2, 3) and reported an antiferromagnetic (AF) ordering of the  $\text{Cr}^{III}$  magnetic moments below  $T_N \approx 30$  K. Much more recently, our neutron diffraction observation of an antipolar copper sublattice below 150 K in this compound (4) suggested that the RT density smearing may be due to the  $\text{Cu}^I$  ion hopping between two off-center sites within its octahedron rather than to a static kind of disorder. The interest in these thiophosphates as a new family of layered ferroelectric-type materials, heightened lately by the discovery of a nearly polar  $\text{Cu}^I$  configuration (3) and ferroelectric behavior (5) in  $\text{CuInP}_2\text{S}_6$ , motivated us to reinvestigate certain aspects of the RT structure of  $\text{CuCrP}_2\text{S}_6$ . Neutron powder diffraction data collected below  $T_N$  also allowed us to determine the magnetic structure of the AF phase.

The RT continuous copper electronic distribution in  $\text{CuCrP}_2\text{S}_6$  was satisfactorily modeled by two quasi-vertically disposed and partially filled positions, one distinctly ( $\text{Cu}1$ ) and the other slightly ( $\text{Cu}2$ ) shifted from the octahedral center (1). A two-fold axis through the octahedron

leads to twice as many possible positions, so that the  $\text{Cu}1$  and  $\text{Cu}2$  occupancy ratios per  $\text{CuS}_6$  unit may be given as 0.66 and 0.34, respectively. Refinement of the copper anisotropic thermal factors revealed appreciable values, with the  $\text{Cu}1$  thermal ellipsoid being elongated perpendicular to the  $[\text{SCu}_{1/3}\text{Cr}_{1/3}(\text{P}_2)_{1/3}\text{S}]$  layer and that of  $\text{Cu}2$  nearly spherical. The probability of finding a copper atom in a volume element, formally called the joint probability density function (jpdf) (6), can be calculated as the weighted sum of the Fourier transforms of the  $\text{Cu}1$  and  $\text{Cu}2$  temperature factors. Moreover, the one-particle potential at a point  $\mathbf{r}$  may be derived as

$$V(\mathbf{r}) = V_0 - k_B T \ln [\text{jpdf}(\mathbf{r})],$$

where  $k_B$  is the Boltzmann constant and  $T$  is the absolute temperature. Because the present case involves underoccupied positions, the diffraction data represents an average filling of these sites and  $V(\mathbf{r})$  is a pseudo rather than a real potential (6). Although the energy values thus obtained should be interpreted with caution, the features of such a pseudo potential remain qualitatively correct.

The copper jpdf and  $V(\mathbf{r})$  were calculated from the structural parameters of Ref. (1) and mapped out using the PROMETHEUS suite of programs (7); Fig. 1 displays the results. It is clear from this that there is no probability density maximum close to the octahedral center, and consequently the pseudo potential has a simple double-well shape. Note that a distance of 2.52 Å, i.e., larger than the diameter of a  $\text{Cu}^I$  ion, separates the two minima. Thus, as may be expected from the unlikelihood of a statically stable and octahedrally coordinated  $\text{Cu}^I$  (8), neither the near-center electronic density peak nor the  $\text{Cu}2$  site corresponds to an equilibrium position. Rather, each may be indicative of a non-zero probability of finding the copper ion between the two potential minima. This is consistent with a thermal hopping model of the copper distribution which says that the RT phase is nonpolar in a

<sup>1</sup> To whom correspondence should be addressed.